

New thermoelectric effect in tunnel junctions

A. D. Smith,* M. Tinkham, and W. J. Skocpol

Department of Physics and Division of Applied Sciences, Harvard University, Cambridge, Massachusetts 02138

(Received 23 June 1980)

A new type of thermoelectric current effect is derived for tunneling through oxide barriers between metals at different temperatures, for both superconducting and normal tunnel junctions. This effect was observed in both current and voltage measurements on Al-PbBi tunnel junctions in which one electrode was heated by laser irradiation. The existence of this thermoelectric effect may resolve long-standing discrepancies between experimental results and theoretical predictions for a series of point-contact experiments.

I. INTRODUCTION

A temperature gradient across a bimetallic superconducting loop is predicted to induce a current flow around the loop, if the quasiparticles have nonzero thermopower S .^{1,2} A number of different experimental designs have been used to look for such an effect, most recently a laser-heated loop experiment by Schuller and Falco,³ and a toroidal geometry experiment by Van Harlingen and Garland.⁴

A second group of experiments has concerned thermoelectric effects caused by interaction of temperature gradients and supercurrents. An effect proportional to $\nabla_s \cdot \vec{\nabla} T$ was predicted⁵ to give rise to a local charge imbalance within the quasiparticles which could be measured with a tunnel junction probe. The magnitude of the effect depends on the mean free path of the quasiparticles, as well as Δ , but is entirely independent of the normal-state thermopower. Experiments by Clarke *et al.*,⁶ and others^{7,8} confirm the existence of an emf which is proportional to $\nabla_s \cdot \vec{\nabla} T$, although the theoretical magnitude and temperature dependence have been open to debate.^{9,10}

This paper will treat an entirely different type of thermoelectric effect, applicable to tunneling through oxide barriers between both superconductors and normal metals. Laser illumination of one film of a tunnel junction was used to create a nonequilibrium situation which can be modeled as a temperature difference across the oxide barrier. Observations of the thermoelectric effect will be presented for both open-circuit voltage measurements and short-circuit current measurements. The existence of this thermoelectric effect can explain discrepancies between experimental results and theoretical predictions in several earlier superconducting thermopower experiments.

II. DERIVATION OF A TUNNELING THERMOELECTRIC CURRENT

The tunneling barriers in tunnel junctions are typically 10–40-Å-thick oxides of one of the electrodes. Moderately thick oxide barriers reduce the transmission probability of electrons to cross the barrier to $\sim 10^{-10}$. The oxide barrier also serves as a barrier to phonon propagation.¹¹ As a result, the metal films comprising the tunnel junction can have significantly different temperatures in nonequilibrium situations.¹² These effects are especially important at low temperatures, when the phonon heat transmission ($\sim T^4$) is low.

Qualitatively the physical processes explaining a thermoelectric quasiparticle current at zero voltage can be seen in Fig. 1, in which the semiconductor-model density of states is plotted for an Al-PbBi tunnel junction. A heat source creates an equal number of electronlike (upper branch) and holelike (lower branch) quasiparticles in the PbBi, so that the superconductor on the left (PbBi) is effectively at a higher temperature than the superconductor on the right (Al). The Fermi energies are held equal externally by a superconducting shorting wire. Electrons tunnel across the barrier from the PbBi to the Al in the tunneling channel labeled *A*. There is a back current, labeled *B*, for states in the lower branch. For an oxide transmission probability $X(E)$ that is energy *independent*, the charge transfer for the two processes exactly cancels. Harrison has noted¹³ that the densities of states of the metals are proportional to $(dE/dk)^{-1}$ and the group velocities for electrons to approach the barrier are proportional to dE/dk , so that the branch cancellation is independent of density of state changes. If transmission probabilities for *A* and *B* processes are *not* exactly equal, however, there *will* be

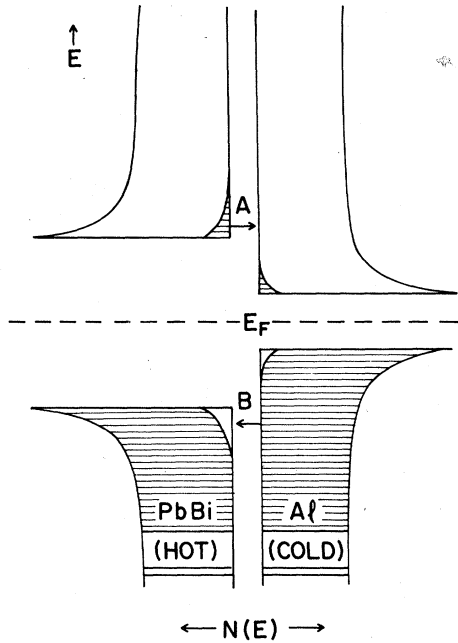


FIG. 1. Semiconductor model of tunneling, shown for an Al-PbBi junction illuminated on the PbBi side.

a net thermoelectric current, which can be experimentally measured by using a galvanometer in place of the superconducting shorting wire.

An estimate of the energy dependence of the electron transmission probability can be obtained using the one-band WKB approximation. For an oxide barrier potential ϕ , electron energy E (both measured from E_F), and oxide thickness s , $X(E)$ is given by¹⁴

$$\ln[X(E)] \cong -\alpha s (\phi - E)^{1/2} + \text{const} \quad (1)$$

where

$$\alpha = 4\pi(2m)^{1/2}/h = 1.025 \text{ eV}^{-1/2} \text{ \AA}^{-1} \quad (2)$$

The dependence of X on the angle of incidence upon the barrier has been integrated out.

We will restrict our analysis to study of tunneling at low voltages, i.e., $V \ll \phi/e$. In this case, only states close to E_F contribute significantly to the tunneling current. The transmission probability for these states may be expressed in terms of a Taylor's expansion about E_F :

$$\ln[X(E)] = -b + c_1 E + \dots \quad (3)$$

The fractional change in X as E varies is given by

$$\frac{1}{X} \frac{dX}{dE} \Big|_{E_F} = c_1 = \frac{d}{dE} \ln(X) \Big|_{E_F} \quad (4)$$

For the model described by Eq. (1) this may be

evaluated as

$$c_1 = \frac{\alpha s}{(2\phi^{1/2})} \cong \frac{23 + \ln(RA)}{2\phi} \quad (5)$$

where R is in ohms and A is in cm^2 .

Typical values of the parameters for an aluminum oxide tunneling barrier would be $s \cong 10 \text{ \AA}$ and $\phi = 3.7 \text{ eV}$.¹⁵ Evaluating Eq. (5) for electron states near the Fermi surface and a 1-ohm cm^2 junction resistivity, this simple model gives

$$c_1 = 3.1 \text{ eV}^{-1} \quad (6)$$

[It should be noted that Gundlach¹⁶ has done calculations using a slightly more sophisticated, two-band model. This model introduces the effects of the valence band of the oxide on the tunneling probabilities. In general the results of these calculations are to lower the estimates of c_1 , although accurate predictions for c_1 are rather difficult. The two-band model has proven superior to the one-band model when applied to explain high voltage asymmetries in tunneling $I(V)$ characteristics.^{17,18}

If the relevant energy separation of the two branches is $2\Delta_{\text{PbBi}} (\cong 3 \text{ meV})$, Eq. (4) suggests that the A currents illustrated in Fig. 1 could be expected to be on the order of 1% larger than the B currents.

The exact magnitude of the current depends on the excess number density of excited quasiparticles that are able to tunnel as well as details of the junction itself. The semiconductor model predicts

$$I_0 = \frac{1}{eRX(0)} \int_{-\infty}^{\infty} X(E) N_1(E) N_2(E) \times [f_1(E) - f_2(E)] dE \quad (7)$$

where I_0 is the predicted zero voltage current, N_i is the superconducting density of states normalized to the electronic density of states per spin, $N(0)$, and e is negative. The normalized transmission probability can be expanded as

$$X(E)/X(0) = 1 + c_1 E + \dots \quad (8)$$

Using this expression in Eq. (7), the first term integrates to zero, leaving

$$I_0 = \frac{1}{eR} c_1 \int_{-\infty}^{\infty} E N_1(E) N_2(E) [f_1(E) - f_2(E)] dE \quad (9)$$

Although the semiconductor model used to describe the phenomena of a thermoelectric current correctly predicts the rough magnitude and correct sign of the effect, it does not carefully take into account the combined hole-electron nature of quasiparticles. (For a more detailed and rigorous calculation of the thermoelectric current, see the Appendix.) The major conclusion should be valid, however, namely, that a thermoelectric current proportional to the excess number of quasiparticles able to tunnel

should be excited across the oxide barrier of the tunnel junction, i.e.,

$$I_0 \propto n - n_0(T) , \quad (10)$$

where n is the number density of quasiparticles [conventionally normalized to $4N(0)\Delta(0)\Omega$], Ω is the electrode effective volume, and $n_0(T)$ is the thermal equilibrium value defined by the counter electrode (A1) effective temperature. [See Appendix equations (A6) and (A7).]

It should be noted that the thermoelectric current derived here is entirely a tunneling barrier effect. The current is independent of those electrode material parameters normally associated with thermoelectricity: the thermopower S , the quasiparticle diffusion length Λ_Q , the mean free path l , etc. The only important material parameters are those determining the number of quasiparticles which are able to tunnel.

For the experiments reported here, a laser was used to supply heat to one of the films comprising the tunnel junction. An advantage of this technique over Joule heating techniques is that it avoids inductive or capacitive coupling between external heaters and the tunnel junction. A difficulty of the laser heating technique is that the effective temperature of the illuminated film, T^* , must be estimated rather than measured directly.

The value $(n - n_0)$ is related to the incident laser power P , as well as the gap parameter. The number of quasiparticles excited may be estimated using the coupled Rothwarf-Taylor rate equations.¹⁹ The steady-state number of excited quasiparticles (in normalized units) is

$$n - n_0 = (P\tau_{\text{eff}})/[4\langle E\rangle\Delta(0)N(0)\Omega] , \quad (11)$$

where τ_{eff} is the effective lifetime of the excitations before recombination occurs and $\langle E\rangle$ is the average energy per quasiparticle.²⁰ The lifetime τ_{eff} is itself dependent on the number of quasiparticles. For a quasiparticle to recombine, it must pair with another quasiparticle. The recombination rate for quasiparticles is simply proportional to the number of combinations of pairs of quasiparticles ($\frac{1}{2}n^2$), so the effective recombination time is given by

$$\tau_{\text{eff}} = n \left(\frac{dn}{dt} \right)^{-1} = b\tau_0\gamma_n , \quad (12)$$

where τ_0 is a characteristic time for the superconductor,²¹ b is a dimensionless constant of proportionality (equal to 0.048), and γ is the phonon trapping factor,¹¹ which may be on the order of 50 depending on the materials at the interface.

If $n \ll 1$, Δ is independent of n , and Eqs. (11) and (12) may be solved self-consistently, yielding

$$n - n_0 = \frac{1}{2} \left(\{ n_0^2 + P\gamma b\tau_0/[\langle E\rangle\Delta N(0)\Omega] \}^{1/2} - n_0 \right) . \quad (13)$$

For small power levels, or large $n_0(T)$, $(n - n_0)$ is linear in the absorbed power, with a coefficient that depends on temperature essentially as $n_0(T)^{-1}$. For high-power absorption at low temperatures, $(n - n_0)$ saturates and is proportional to $P^{1/2}$.

III. NORMAL-METAL TUNNELING

For the special case that both metals are normal, the zero-voltage thermoelectric current may be calculated explicitly. For a tunnel junction with side 1 at temperature T_1 and side 2 at temperature T_2 , the current at zero voltage may be calculated by direct integration of Eq. (9). Then

$$I_0 = (1/eR)c_1 \left(\frac{1}{6}\pi^2 \right) k_B^2 (T_1^2 - T_2^2) . \quad (14)$$

For a 1-ohm cm^2 junction with a barrier height of 3.7 eV,¹⁵ Eq. (14) predicts a current:

$$I_0 R = -8.3 \times 10^{-8} (T_1^2 - T_2^2) , \quad (15)$$

where $I_0 R$ is measured in volts and T is measured in kelvin. In the limit of small temperature differences across the barrier, this is

$$I_0 R = -1.7 \times 10^{-7} T dT . \quad (16)$$

Of course, actually to measure this current, or the open-circuit voltage for a tunnel junction, care must be taken to recognize the Seebeck thermoelectric emf's within the metals themselves. Although the oxide thermoelectric effect increases at higher temperatures, the higher thermal conductivity makes maintenance of a large thermal gradient more difficult. In a superconductor, on the other hand, the existence of a gap can serve to slow relaxation to thermal equilibrium, thus making a fairly large temperature difference possible. More critically, in a superconductor the existence of supercurrent flow at constant-pair electrochemical potential allows one actually to maintain the equality of the electrochemical potential across the junction, which is assumed in making this model.

IV. EXPERIMENTAL PROCEDURE

A. Voltage measurements

Two experiments were performed to measure the thermoelectric current through the oxide. In the first experiment, Al-PbBi tunnel junctions were formed using standard techniques, which are described in more detail in an earlier paper.²² Dirty aluminum films were evaporated onto single-crystal sapphire substrates to a thickness of 1000 Å and were oxidized in 0.1 Torr of oxygen for 1 min. Next a 1500-Å-thick layer of $\text{Pb}_{0.95}\text{Bi}_{0.05}$ was deposited, forming a

junction with an area of 1.5 mm^2 and normal-state resistance of tens of ohms. T_c of the dirty aluminum was $2.2 \pm 0.2 \text{ K}$. The junctions were immersed in superfluid helium in a Dewar with transverse optical access.

A schematic diagram of the experiment is shown in Fig. 2. An argon laser beam chopped at 337 Hz provided heat to the PbBi side of the junction. The relatively poor phonon coupling between the two films allowed the PbBi film to reach a temperature significantly above that of the Al film, which remained near the bath temperature. (The electron temperature rises were estimated by observing the changes in the gaps of the two films as the laser was turned on.)

The tunnel junctions were biased at constant current for several voltages and temperatures. The laser-induced voltage change, dV , was detected synchronously and digitally recorded as a function of voltage. Both the in-phase (0°) and out-of-phase (90°) components of dV were tabulated in order to check for shifts in phase of the signal. Junction capacitance did introduce phase shifts and some attenuation, but these were readily corrected out by multiplying the measured magnitudes of dV by the secant of the measured phase shift.

There are two observable effects of laser illumination. The first is a general increase in the tunneling conductance, caused by the larger number of excited quasiparticles (see Ref. 22). For constant-current biasing, this leads to a contribution to the observed $|dV|$ which is an even function of voltage, and is defined as the symmetric contribution. [The measured $dV(V)$ reverses sign near the origin.] Of more concern here, is the thermoelectric contribution to $|dV|$ which is antisymmetric in V . The thermoelectric current through the tunneling barrier should be only

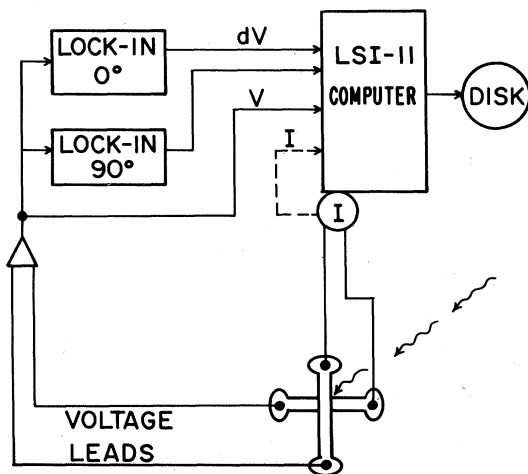


FIG. 2. Schematic diagram for voltage measurements. The current through the tunnel junction could be controlled externally.

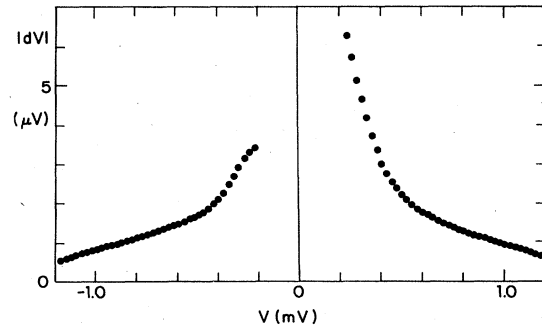


FIG. 3. Observed values of $|dV|$ vs V for an Al-PbBi tunnel junction illuminated on the PbBi side. The temperature was 1.588 K.

weakly voltage dependent, as is clear from the argument leading to Eq. (5). For a fixed-current bias, the thermoelectric current, I_0 , must be countered by a decrease in the conventional quasiparticle current. This gives rise to an observable shift in the junction voltage given by

$$dV = \frac{dV}{dI} I_0, \quad (17)$$

where dV/dI is the dynamic resistance of the tunnel junction.

Typical behavior of $|dV|$ is shown in Fig. 3. The absolute value of dV is plotted to show the asymmetry, especially at low voltages. The observed voltage shift $|dV(V)|$ could be decomposed into a symmetric $dV^s(V)$, and an antisymmetric $dV^a(V)$. The measured antisymmetric contribution is plotted in Fig. 4. The falloff in dV^a for large voltages corresponds to the decrease in the dynamic resistance of the tunnel junctions at high voltages expected from Eq. (17). Figure 5 shows the asymmetry plotted as a function of the dynamic resistance of the junction for one tunnel junction at a fixed temperature. The

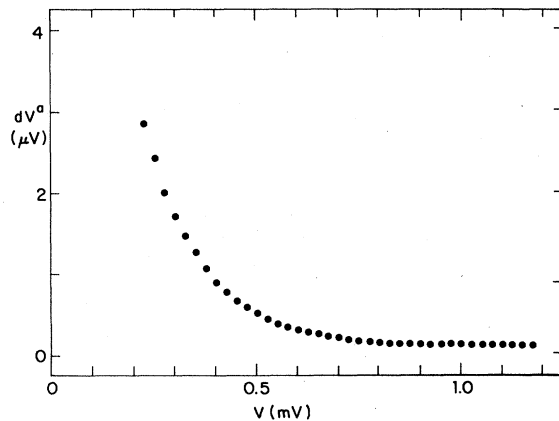


FIG. 4. Measured dV^a vs V for data shown in Fig. 3.

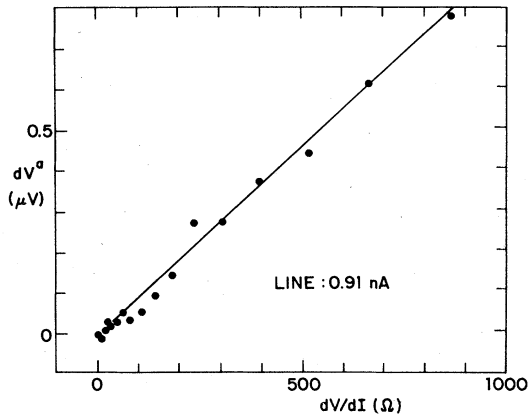


FIG. 5. Observed dV^a vs dV/dI . The bath temperature was 1.78 K. The straight line is the best fit to a constant thermoelectric current model.

straight-line fit, corresponding to a constant thermoelectric current of $I = 0.91$ nA, is good to within the accuracy of the data.

B. Current measurements

In order to study further the temperature and power dependence of the thermoelectric effect, a more direct method of measuring the thermoelectric current was devised. To measure currents of pA at low voltages, it was necessary to use a superconducting quantum interference (SQUID) system as a highly sensitive, low-noise galvanometer. The experimental system is shown schematically in Fig. 6. Tunnel

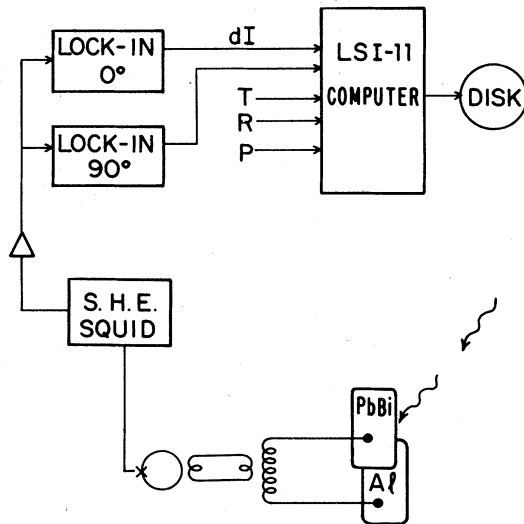


FIG. 6. Schematic diagram for current measurement of the thermoelectric effect. The bath temperature, laser output power, and resistance of an Al strip were monitored in addition to I_0 .

nel junctions were made with areas of about 5 mm^2 , somewhat larger than in the earlier experiment. In addition to the tunnel junction, the substrates contained an evaporated Al strip, used for determining T_c of the Al film of the tunnel junction. As before, the junctions were immersed in the helium bath. No voltage leads or external current leads were attached to the tunnel junction. Laser illumination induced a thermoelectric current out of the tunnel junction. A superconducting transformer with a current gain of 14 coupled the tunnel junction to a S.H.E. SQUID system. The SQUID output was detected synchronously using the two-lock-in scheme described earlier. The bath temperature was measured using a germanium resistance thermometer near the sample. Measurements of I_0 , the temperature, laser power, and Al strip resistance were taken simultaneously and digitally recorded.

The necessity of using the highly sensitive SQUID and a high-power argon-ion laser presented special problems in noise shielding. The difficulties were overcome by the use of a Corning graded-index glass optical fiber to couple the laser radiation to the tunnel junction. The argon laser beam was focused down to excite one end of the fiber. The fiber ran down the hall, into an rf shielded room, through a vacuum seal, and down into the liquid helium, where the output beam illuminated a spot on the tunnel junction.

Results for a sweep in temperature, with constant (low) laser power, are shown in Fig. 7. The sample temperature was initially at 3 K and the temperature was reduced eventually to roughly 1.6 K. The current became larger as T [and hence $n_0(T)$] de-

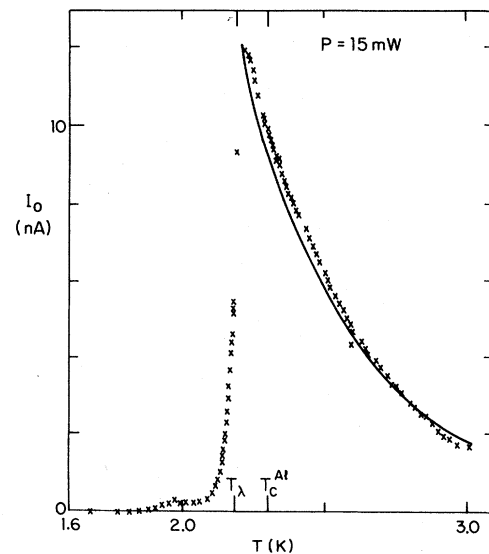


FIG. 7. Observed $I_0(T)$ for an Al-PbBi tunnel junction, illuminated on the PbBi side. The laser power was held fixed at 15 mW.

creased, as expected from Eq. (13). There was no noticeable change observed upon passing through T_c of the dirty aluminum film. The solid curve is proportional to $n_0(T)^{-1}$, as our model predicts. The fit is good for temperatures above the λ point of helium. At the λ point there was an abrupt decrease in the measured signal. This was due to the improved coupling of phonons to the now superfluid bath, and the resultant decrease in τ_{eff} . At a temperature near 1.85 K the signal disappeared to the limits of resolution (1 pA) of the experiment. This temperature corresponded to that at which the Josephson supercurrent became large enough to be observed in a separate experiment in which current and voltage leads were attached to the sample. Accordingly, we interpret the disappearance of the *external* thermoelectric current as due to its being effectively shorted out by an *internal* backflow of supercurrent. This interpretation is supported by the fact that at nonzero voltages, where there is no dc supercurrent, a thermoelectric current is measured in the experiments reported in Sec. IV A, even at temperatures as low as 1.5 K.

The SQUID galvanometer experiment was also performed at fixed temperature while varying the laser power P . Figure 8 shows the power dependence of I_0 for several temperatures. As expected, the observed currents become nonlinear in power for the lower temperatures.

Figure 9 shows the predictions for our simple model [Eq. (13)]. The value of c_1 and the value of the phonon-trapping factor have been adjusted to give a best fit. For an assumed film optical absorptivity of 2%, and τ_0 of 4.3×10^{-11} sec, the fit value of γ is 15. The fit value of c_1 was an order of magni-

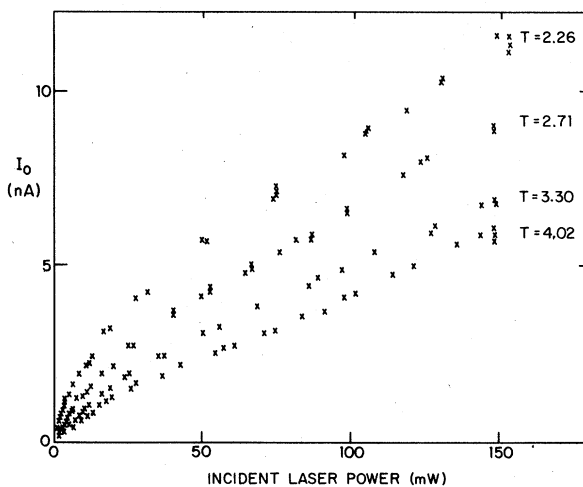


FIG. 8. $I_0(P)$ for four different fixed temperatures. As expected the thermoelectric current is more nearly linear in power for higher temperatures, but proportional to $P^{1/2}$ for lower temperatures. The fit to square-root dependence for low temperatures was quite good.

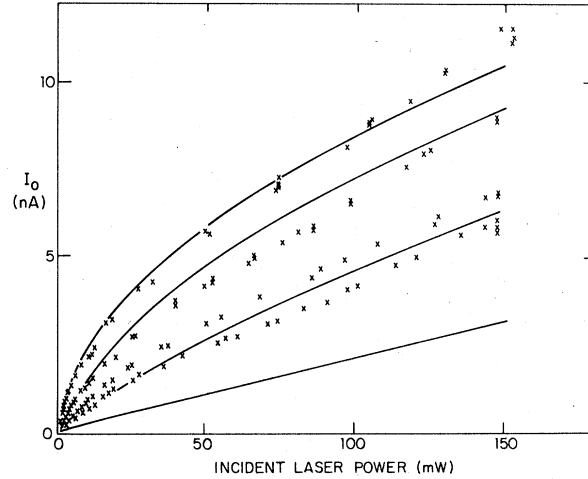


FIG. 9. Predicted $I_0(P)$. Two fitting parameters have been adjusted to attempt to fit all four curves.

tude less than predicted by the one-band-model calculation [Eq. (5)], but was in qualitative agreement with the two-band corrections proposed by Gundlach.¹⁶ While the general magnitude and shape of the $I_0(T)$ curves are in good agreement with the simple Rothwarf-Taylor calculations done here, the exact temperature dependence was less satisfactory. No attempt has been made to include liquid-helium effects which would cause a temperature dependence to the phonon-trapping factor. Available literature suggests that heat transport through helium is strongly dependent on the exact sample geometry and surface structure, and is therefore difficult to calculate realistically. The importance of the liquid helium in determining phonon trapping factor is evidenced by the dramatic decrease in I_0 as the helium becomes superfluid.

V. COMPARISONS WITH OTHER EXPERIMENTS

The existence of a thermoelectric current across tunneling junctions can explain several discrepancies between earlier experiments and existing theory. In particular, it is useful to examine the experiments of Clarke and Freake²³ in light of temperature gradients across oxide barriers. Their experiment consisted of a point contact formed by bringing a sharpened Pb wire into contact with a Pb foil. The temperatures of the wire and the foil could be independently varied and measured. Although the point-counter supercurrent effectively shorted out any thermoelectric current, it was possible to measure the difference in the magnitude of the critical current for the two directions of current flow. This asymmetry was interpreted in terms of a thermoelectric quasiparticle current. Clarke and Freake measured a sizable

current whenever the point and foil were at different temperatures, although the size of the effect varied over a factor of 50 for different point contacts. The existence of any asymmetry current was surprising to those who expected no steady-state thermoelectric current to be possible within a superconducting channel.

In an effort to clarify matters, Welker and Bedard²⁴ performed a somewhat similar experiment using Nb wire. They were extremely careful about sample preparation conditions. For very clean, oxide-free point contacts, where a small but continuous superconducting channel could be assumed to exist, they found no evidence for a thermoelectric current. If they allowed an oxide to form in the point-contact area, however, they did note a significant thermoelectric current. The deduced current was in the same direction relative to the temperature difference as was observed by Clarke and Freake, although Nb and Pb have thermopowers which differ in sign. Thus, the thermoelectric voltage was of the wrong sign to be predicted by the thermopower arguments of Clarke and Freake, but is correctly predicted by our model.

A follow-up experiment by Matsinger *et al.*²⁵ was performed using both Nb and Pb point contacts. Asymmetry was looked for over the entire $I(V)$ curve of the point contacts, for both directions of applied temperature gradient. For situations where one electrode was raised above its T_c , while the other electrode was superconducting, they measured the expected normal thermopower. With both metals below T_c no asymmetry was observed to the limit of their sensitivity. Matsinger *et al.* concluded that the Clarke and Freake measurements were "caused by a surface layer," and were not an intrinsic superconducting effect.

It seems likely that the asymmetric critical currents measured both by Clarke and Freake and by Welker and Bedard are the result of thermoelectric currents across oxide barriers. The sign predicted here for tunneling-barrier thermoelectric currents agrees with experimental results. The magnitude of the predicted effect can be calculated using the point-contact parameters given in the Clarke and Freake paper. Integrating Eq. (7) numerically for Pb electrode temperatures of 7.0 and 5.3 K gives

$$I_0 = (2/eR)c_1(0.08\Delta^2), \quad (18)$$

where Δ is the lead gap at 5.3 K. Estimating c_1 is not as simple as for our experimental geometry. For Pb tunnel junctions, Basavaiah *et al.* have measured the oxide barrier height as 1.05 eV.¹⁷ The actual junction area is somewhat poorly defined for a point contact. If a $1\text{-}\mu\text{m}^2$ area is assumed, and the junction resistance is 1 ohm, then $c_1 \cong 4 \text{ eV}^{-1}$ and

$$I_0^{\text{theor}} = 0.7 \mu\text{A}. \quad (19)$$

If the junction effective area is larger, the prediction

is logarithmically larger. If not all the temperature difference occurs at the oxide, a smaller I_0 should result. Given the variance in the experimental results, uncertainties in several of the barrier parameters, especially A and ϕ , and the tendency of the one-band approximation to overestimate c_1 , this theoretical value is in good agreement with the plotted Clarke and Freake result

$$I_0^{\text{expt}} = 0.265 \mu\text{A}. \quad (20)$$

(Note that their experimental result has been adjusted by a factor of 2 because the published values are peak to peak.) Coincidentally, the expected normal-state thermoelectric current for the point contact is the same order of magnitude, $0.4 \mu\text{A}$. The two mechanisms are entirely independent; the mechanism reported here is an oxide effect, dependent on the barrier height and thickness, while the Seebeck effect depends on the metallic density of states of the electrode materials.

VI. SUMMARY

For nonequilibrium situations in which a temperature difference exists across a tunneling barrier, we have shown the existence of a thermoelectric current, which exists even with no voltage difference across the oxide. This current results from the energy dependence of the electronic tunneling probability for barrier penetration, and is largely independent of material parameters of the electrode materials. We have measured this thermoelectric effect in an open-circuit experiment as well as with a current measurement scheme. In both cases the data are in at least qualitative agreement with theoretical predictions.

The existence of the tunneling thermoelectric current may explain the supercurrent asymmetries studied in point-contact experiments by a number of authors. The theory presented here correctly predicts the sign and order of magnitude for these asymmetries, as well as the absence of any asymmetry in very clean point contacts.

ACKNOWLEDGMENTS

We wish to acknowledge valuable discussions with Dr. T. M. Klapwijk and Dr. L. N. Smith. The optical fiber used in the experiments was donated by Corning Glassworks. The research was supported by the National Science Foundation under Grant No. DMR-79-04155 and the Joint Services Electronics Program under Contract No. N00014-75-C-0648.

APPENDIX

To calculate correctly the current through a superconducting tunnel junction, it is necessary to take ac-

count of the coherence factors which describe the quasiparticle wave functions. Barrier transmission probability amplitudes T_{kq} describe coupling between states with momenta k in one metal, and q in the other metal. For weak coupling through the oxide barrier, we can assume the familiar tunneling Hamiltonian of the form

$$\mathcal{H}_T = \sum_{k,q} T_{kq} c_k^* c_q + T_{qk}^* c_q^* c_k, \quad (\text{A1})$$

$$\mathcal{H}_T = \sum [T_{kq} (u_k \gamma_{ek0} + v_k \gamma_{hk1}) (u_q \gamma_{eq0} + v_q \gamma_{hq1}) + T_{qk}^* (u_k \gamma_{ek0} + v_k \gamma_{hk1}) (u_q \gamma_{eq0} + v_q \gamma_{hq1})] . \quad (\text{A2})$$

The Hamiltonian consists of eight terms, which fall into two categories. There are four terms involving one creation and one annihilation operator. These terms describe tunneling of quasiparticles from one side of the film to the other. The other four terms each have either two creation or two annihilation operators, and describe pair-breaking or pair-forming

where c_q annihilates an *electron* from the q side of the junction. The sum is taken over electron spins as well as momenta.

The tunneling Hamiltonian must be rewritten in terms of quasiparticle states in order to compute the allowed tunneling current in the superconducting case. Following the notation of Tinkham²⁶

tunneling processes.

For simplicity we will restrict our attention to the case that $eV < (\Delta_k + \Delta_q)$. In this situation pair-breaking and pair-forming tunneling is prohibited by conservation of energy.

By "Fermi's golden rule," the quasiparticle current is simply²⁷

$$I_{qp} = \frac{4\pi e}{\hbar} \sum \int_0^\infty dE |T_{kq}|^2 \{ v_k^2 v_q^2 N_k(E) N_q(E + eV) [f_k(E) - f_q(E + eV)] - u_k^2 u_q^2 N_k(E) N_q(E - eV) [f_k(E) - f_q(E - eV)] \} . \quad (\text{A3})$$

The sum is over both excitation branches for both films (four terms). The sum over spins contributes a factor of 2, which has been incorporated into the equation. The terms involving $u_k^2 u_q^2$ describe the probability of tunneling of electron excitations from the k -side film to the q -side film, shown as A -type processes in Fig. 1. The $v_k^2 v_q^2$ terms involve transferring charge in the other direction (i.e., B -type hole tunneling).

To simplify the calculations further, we will study the special case of zero-voltage current for a normal-metal-insulator-superconductor (N - S) tunnel junction ($V = 0$ and $\Delta_q = 0$). Under these restrictions, Eq. (A3) may be reduced by performing the sum over the electron and hole branches of the normal metal using the values:

$$u_q = \begin{cases} 0, & q < q_F \\ 1, & q > q_F \end{cases}, \quad (\text{A4})$$

$$v_q = \begin{cases} 1, & q < q_F \\ 0, & q > q_F \end{cases}.$$

Therefore

$$I_0^{N-S} = \frac{4\pi e}{\hbar} \sum \int_\Delta^\infty dE (|T_{kq}|^2 v_k^2 - |T_{kq}|^2 u_k^2) \times N_k(E) [f_k(E) - f_q(E)] . \quad (\text{A5})$$

The sum now is only over the $k > k_F$ and $k < k_F$ branches of the superconductor. As was the case be-

fore, the u_k^2 terms describing tunneling from electronlike states in the superconductor, through the oxide, and into the normal metal with an energy E above the Fermi surface. For this electron tunneling it will be assumed that to lowest order in the energy (measured from the Fermi energy)

$$\left| \frac{T_{kq}}{T(0)} \right|^2 = 1 + c_1 E, \quad q > q_F, \quad (\text{A6})$$

where $T(0)$ is the tunneling probability amplitude at the Fermi surface. Similarly for hole tunneling (v_k^2 terms)

$$\left| \frac{T_{kq}}{T(0)} \right|^2 = 1 - c_1 E, \quad q < q_F. \quad (\text{A7})$$

Substituting these values for T_{kq} into Eq. (A5) yields

$$I_0^{N-S} = (4\pi e/\hbar) |T(0)|^2 \times \sum \int_\Delta^\infty dE c_1 E (v_k^2 + u_k^2) \times N_k(E) [f_k(E) - f_q(E)] . \quad (\text{A8})$$

Using the identity ($v_k^2 + u_k^2 = 1$), we can eliminate the dependence on coherence factors in Eq. (A8). The sum over the $k > k_F$ and $k < k_F$ branches then simply introduces a factor of 2, leaving

$$I_0^{N-S} = 2[(4\pi e/\hbar) |T(0)|^2] c_1 \times \int_\Delta^\infty dE E N_k(E) [f_k(E) - f_q(E)] . \quad (\text{A9})$$

The factor $[(4\pi e/\hbar)|T(0)|^2]$ may be replaced by $(1/eR)$.

Several limiting cases of Eq. (A9) are worthy of note. If both electrodes are at the same temperature, there will be no net current flow. On the other hand, if the q -side film is at zero temperature ($f_q = 0$), Eq. (A9) reduces to the not-too-surprising result

$$I = \frac{2}{eR} c_1 \int_{\Delta}^{\infty} dE E N_k(E) f_k(E) \quad (\text{A10})$$

$$= \frac{2}{eR} c_1 \Delta \langle E_k \rangle n_k, \quad (\text{A11})$$

where $\langle E_k \rangle$ is the average quasiparticle energy in the k -side film and n_k is the normalized quasiparticle density.

If the quasiparticle occupation of the k -side film is a Fermi-Dirac distribution with temperature T_k , and the q -side film has temperature T_q then the integral of (A9) can be expressed as a sum of modified

Bessel functions. Then

$$I_0^{N-S} = \frac{2}{eR} c_1 \Delta^2 \times \sum_{m=1}^{\infty} (-1)^{m+1} \left[K_0 \left(\frac{m\Delta}{kT_k} \right) + \left(\frac{kT_k}{m\Delta} \right) K_1 \left(\frac{m\Delta}{kT_k} \right) - K_0 \left(\frac{m\Delta}{kT_q} \right) - \left(\frac{kT_q}{m\Delta} \right) K_1 \left(\frac{m\Delta}{kT_q} \right) \right] \quad (\text{A12})$$

The series converges rapidly at low temperatures. The leading low-temperature behavior is

$$I_0^{N-S} \cong [(kT_k/\Delta)^{1/2} \exp(-\Delta/kT_k) - (kT_q/\Delta)^{1/2} \exp(-\Delta/kT_q)] \quad (\text{A13})$$

The more general case of tunneling between two superconductors can be calculated in a manner similar to that used to derive Eq. (A9). For voltages not large enough to break pairs [$eV < (\Delta_k + \Delta_q)$]

$$I_{\text{qp}} = \frac{1}{eR} \int_0^{\infty} dE \left\{ [1 + c_1(E + \frac{1}{2}eV)] N_k(E) N_q(E + eV) [f_k(E) - f_q(E + eV)] - [1 - c_1(E - \frac{1}{2}eV)] N_k(E) N_q(E - eV) [f_k(E) - f_q(E - eV)] \right\} \quad (\text{A14})$$

The $\frac{1}{2}eV$ terms account for energy gain (or loss) of the electron as it traverses the oxide barrier in the presence of an electric field. Generally the thermoelectric contribution to the current is only slightly voltage dependent. The coefficient c_1 is only weakly voltage dependent,¹⁶ and can generally be treated as a constant for low voltages.

In all cases examined here, the basic temperature dependence is well described by the approximation made in Eq. (10).

*Current address: Dept. of Physics, University of Calif., Berkeley, Calif. 94720.

¹Yu. M. Gal'perin, V. L. Gurevich, and V. I. Kozub, *Zh. Eksp. Teor. Fiz.* **60**, 1387 (1974) [*Sov. Phys. JETP* **39**, 680 (1974)].

²J. C. Garland and D. J. Van Harlingen, *Phys. Lett.* **47A**, 423 (1974).

³I. K. Schuller and C. M. Falco, *Fiz. Nizk. Temp.* **4**, 939 (1978) [*Sov. J. Low Temp. Phys.* **4**, 446 (1978)].

⁴D. J. Van Harlingen and J. C. Garland, *Solid State Commun.* **25**, 419 (1978).

⁵C. J. Pethick and H. Smith, *Phys. Rev. Lett.* **43**, 640 (1979).

⁶J. Clarke, B. R. Fjordbøge, and P. E. Lindelof, *Phys. Rev. Lett.* **43**, 642 (1979).

⁷D. J. Van Harlingen, *Bull. Am. Phys. Soc.* **25**, 411 (1980).

⁸D. F. Heidel and J. C. Garland, *Bull. Am. Phys. Soc.* **25**, 411 (1980).

⁹J. Clarke and M. Tinkham, *Phys. Rev. Lett.* **44**, 106 (1980).

¹⁰A. Schmid and G. Schön, *Phys. Rev. Lett.* **43**, 973 (1979).

¹¹S. B. Kaplan, *J. Low Temp. Phys.* **37**, 343 (1979).

¹²R. G. Melton, J. L. Paterson, and S. B. Kaplan, *Phys. Rev. B* **21**, 1858 (1980).

¹³W. A. Harrison, *Phys. Rev.* **123**, 85 (1961).

¹⁴T. E. Hartman, *J. Appl. Phys.* **35**, 3283 (1964).

¹⁵M. K. Konkin and J. G. Adler, *J. Appl. Phys.* **50**, 8125 (1979).

¹⁶K. H. Gundlach, *J. Appl. Phys.* **44**, 5005 (1973).

¹⁷S. Basavaiah, J. M. Eldridge, and J. Matisoo, *J. Appl. Phys.* **45**, 457 (1974).

¹⁸H. Ekruat and A. Hahn, *J. Appl. Phys.* **51**, 1686 (1980).

¹⁹A. Rothwarf and B. N. Taylor, *Phys. Rev. Lett.* **19**, 27 (1967).

²⁰W. H. Parker, *Phys. Rev. B* **12**, 3667 (1975).

²¹S. B. Kaplan, C. C. Chi, D. N. Langenberg, J. J. Chang, S. Jafarey, and D. J. Scalapino, *Phys. Rev. B* **14**, 4854 (1976).

²²A. D. Smith, W. J. Skocpol, and M. Tinkham, *Phys. Rev. B* **21**, 3879 (1980).

²³J. Clarke and S. M. Freake, *Phys. Rev. Lett.* **29**, 588 (1972).

²⁴N. K. Welker and F. D. Bedard, in *SQUID: Superconducting Quantum Interference Devices and Their Applications*, edited by H. D. Hahlbohm and H. Lübbig (Walter de Gruyter, New York, 1977), p. 200.

²⁵A. A. J. Matsinger, R. de Bruyn Ouboter, and H. van Beelan, *Physica* **93B**, 63 (1978).

²⁶M. Tinkham, *Phys. Rev. B* **6**, 1747 (1972).

²⁷L. N. Smith, Ph.D. thesis (1975) (unpublished).